QUANTITATIVE ANALYSIS OF THREE ATMOSPHERIC CORRECTION MODELS FOR AIRBORNE VISIBLE/INFRARED IMAGING SPECTROMETER (AVIRIS) DATA

J.M. van den Bosch
Geography Department
University of California
Santa Barbara, CA

R.E. Alley
Jet Propulsion Laboratory
California Institute of Technology
Pasadena, CA

Abstract. Current atmospheric correction models applied to imaging spectroscopy data include such methods as residual or scene average, flat field correction, regression or empirical line algorithm, the continuum interpolated band ratio (CIBR) and LOWTRAN 7. Due to the limitations of using residual and flat field corrections on vegetated scenes, three methods will be compared: regression, CIBR and LOWTRAN 7. Field-measured bright and dark targets taken at the time of the 13 April 1989 AVIRIS scene of Jasper Ridge, California were used to formulate the regression method atmospheric correction. Using this corrected scene as "ground truth," the CIBR and the LOWTRAN 7 methods are compared on the vegetated scene.

Three spectra were chosen for comparison: representative samplings of two vegetation types (chaparral and an irrigated crop) and water in the Upper Crystal Springs Reservoir. Correlation and root median squared (RMS) differences were calculated for the atmospherically corrected spectra.

Overall, CIBR and LOWTRAN 7 with radiosonde data were highly correlated and had low RMS differences. LOWTRAN 7 with radiosonde input showed closer agreement with the regression method (assumed "ground truth") than CIBR. It appears that CIBR and LOWTRAN 7 can approach fairly realistic atmospheric corrections for a vegetated AVIRIS scene. Accuracy of both CIBR and LOWTRAN 7 corrections is affected by the estimation of water vapor in the air. When assuming regression represents "ground truth," several possible sources of error can be introduced.

I. Introduction

Imaging spectrometers such as AVIRIS have been used to detect, identify and quantify ecosystems subject to changes from a local and regional scale to a global scale. The high spectral resolution of AVIRIS data with its contiguous 10 nm wide bandwidths from 0.4–2.5 μm coupled with 20 m spatial resolution allows analyses of general ecosystem characteristics such as net photosynthesis (biomass), indicators of plant productivity and stress (chlorophyll, nitrogen, leaf water absorption), nutrient availability (starch, sugar), and rate of litter decomposition (lignin, cellulose), which may serve as temporal and spatial precursors of change. Investigations of the subtle shifts in the slope of the red edge and the position and depth of absorption features in vegetation spectra require careful application of atmospheric corrections in order to extract such detailed information and also to allow comparisons of multidate imagery for phenological studies.

II. Methodology

Based on the limitations posed by the residual/log residual (or scene average) and flat field atmospheric corrections on a vegetated AVIRIS scene as discussed by van den Bosch and Alley

(1990), the regression, LOWTRAN 7 and CIBR methods were compared. A horizontally homogeneous atmosphere and a small elevation variation (El_{Δ}=101m) within the scene were assumed in all of the atmospheric correction models.

The 13 April 1989 AVIRIS image was radiometrically corrected by Jet Propulsion Laboratory (JPL). Three calibration targets (including one bright and one dark target) were used to develop linear relationships between the digital radiance data and the surface reflectance. This regression method has been described in detail (Elvidge, 1988; Elvidge and Portigal, 1990).

LOWTRAN is a model and computer code that can be used to predict spectral radiance for various viewing geometries and atmospheric conditions. The model was developed by the Air Force Geophysics Laboratory in 1972. The latest version, LOWTRAN 7, was released in 1989 and includes multiple scattering, desert aerosol haze type, and a more detailed model of trace gases (Kneizys et al., 1990).

The LOWTRAN 7 method was applied to radiometrically corrected data with input profiles of atmospheric pressure, temperature, and moisture content (dewpoint) as a function of altitude provided by radiosonde data. The viewing geometry was determined by the sensor altitude, target elevation, and solar zenith angle computed by LOWTRAN as a derivation of Julian day, time, latitude and longitude. A variable visibility override was given to the user-designated (radiosonde) geographical model atmosphere with the rural, 23 km visibility aerosol haze model. The observer visibility, V_{obs}, was converted (Kneizys et al., 1990) to meteorological range, V, as follows

$$V = 1.3 * V_{obs} \quad (1)$$

where V_{obs} = 20 km, as reported by ground observation

The second input mode for the LOWTRAN 7 method utilized ground meteorological data collected at the time of the overflight. These parameters included air temperature and visibility combined with the default conditions of the rural, mid-latitude summer model. Both the ground and radiosonde input modes assumed a spectrally constant reflectance (0.15, in this case) and LOWTRAN was used to model the expected radiance when viewing such a surface. By applying a gain and an offset derived from the LOWTRAN results, spectral reflectance was computed (van den Bosch and Alley, 1990).

The CIBR is a ratio between an estimated continuum radiance at the 940 nm water absorption band center derived by linear interpolation between out-of-band continuum radiances to either side and the actual absorption band radiance at the 940 nm wavelength of maximum absorption. The CIBRs are calibrated using LOWTRAN 7 to yield

$$CIBR = \exp(-\alpha w^{\beta}) \quad (2)$$

where w = path precipitable water in g/cm^2

α and β = constants specific to 940 nm band

After calculating the CIBR for the whole scene to recover the total column abundance of water from the atmosphere, the values obtained can then be related to the amount of water present in the scene by running LOWTRAN for varying amounts of water (between zero and twice the normal amount for the atmospheric condition of the overflight). Assuming a constant background reflectance (0.15), the CIBRs can be related to the water predicted by LOWTRAN for each pixel and then corrected to reflectance (Carrere, 1991; Carrere et al., 1991; Conel and Carrere, 1991; and Green et al., 1989).

Three target spectra were chosen: two vegetation types (chaparral and an irrigated crop) and water from the Upper Crystal Springs Reservoir. Statistics generated on the atmospherically corrected spectra include correlation and root **median** squared difference, RMS. The median squared difference was utilized rather than the mean squared difference due to the fact that the median variance was smaller than the mean variance; therefore, the median was a more efficient way of characterizing the data. This also was a protection against outliers.

III. Discussion

The corrected spectra along with the corresponding uncorrected spectra are plotted on the same graph with a 20% offset. The discontinuities in the spectra occur at the major water absorption bands. All of the corrected spectra exhibit a pronounced spike in the 0.400–0.440 μm range that is an artifact of the applied radiometric calibration. This spike can also be seen in the uncorrected spectra.

Figure 1 is an 18 pixel average of an irrigated crop. The chaparral in Figure 2 is dominated by *Adenostema fasciculatum*, a drier, south facing component of the chaparral community. The shape of all three corrected spectra (Figures 1 and 2) in the A spectrometer (0.400–0.700 μm) is very similar with a peak at 0.55 μm. The slope of the red edge at 0.700–1.1 μm in the B spectrometer (0.700–1.200 μm) shows agreement among the spectra with the height of the shoulder varying. The vegetation spectra in the C and D spectrometers (1.200–1.800 and 1.800–2.450 μmi, respectively) are markedly similar in shape. Since the crop and chaparral spectra resemble each other, the statistics were averaged (Figure 5a and 5b).

Overall, Figure 5a shows LOWTRAN 7 with radiosonde data has a higher correlation with the regression method than CIBR in all four spectrometers. However, both CIBR and LOWTRAN 7 have fairly high RMS when compared with the regression spectrum. Figure 5b compares CIBR v. LOWTRAN 7 radiosonde and CIBR v. LOWTRAN 7 ground data. Both LOWTRAN input models show high correlation with CIBR in the A and D spectrometers accompanied by low RMS. However in the B and C spectrometers, the ground input mode has a negative correlation with CIBR and a higher RMS.

Figure 3 represents a single pixel of water in the deepest part of Upper Crystal Springs Reservoir within the image boundary. All three atmospheric correction models are similar. Figure 4 compares the two input modes for the LOWTRAN 7 correction. Using the defaults of the LOWTRAN radiative transfer models in general overcompensates for the 0.94 and 1.15 μm water absorption features. Aside from the aforementioned deviation, the ground meteorological input spectrum resembles the radiosonde spectrum. The statistical analysis for regression v. CIBR and LOWTRAN 7 with radiosonde shows higher correlation in the A and D spectrometers and relatively large RMS in all four spectrometers (Figure 5c). The results of CIBR compared to both input modes of LOWTRAN 7 demonstrate the same trends (Figure 5d) as the vegetation spectra in Figure 5b.

IV. Sources of Error

As noted, there is a spike centered at approximately 0.420 μm that is associated with the 1989 calibration file. The regression method reduced this spike, while the LOWTRAN 7 and CIBR methods did not.

There are problems associated with the assumption that the regression method represents "ground truth." The vegetation spectra (Figures 1 and 2) should exhibit pronounced leaf water

absorption features located at 0.95 and 1.15μm because the imagery was acquired in the spring. However, the regression spectra are almost featureless in the B (0.670–1.290 μm) and C (1.250–1.870 μm) spectrometers. The question remains as to how deep the leaf water absorption feature should be in "reality."

A source of concern in applying the regression method is how well the laboratory or field measured reflectances represent the standard targets (Conel et al., 1988). Another source of concern is the choice of bright and dark targets. When the polo fields were used as the bright target, "anti-vegetation" peaks were introduced at the leaf water absorption features (Figure 6). The regression method was reformulated using a parking lot as the bright target. The minimal criterion for separation of the dark and bright targets should be at least 20%.

The LOWTRAN spectra exhibit more sensitivity to errors in the moisture content than to any other parameter, which may be related to the inaccuracies of radiosonde data (Bruegge et al., 1990). Sources of error for CIBR are also linked to retrieval of atmospheric water vapor and are discussed at length by Carrere (1991) and Conel and Carrere (1991).

V. Conclusions

The specific feature of interest may influence the choice of atmospheric correction. In the A spectrometer, the main absorption features are the chlorophyll a and b wells (a - 0.440 and 0.663 μm; b - 0.460 and 0.640 μm). There is close agreement among the regression method, CIBR and both input modes of LOWTRAN 7. However, the calibration spike affects the chlorophyll as well at 0.440 μm.

The red edge and the near infrared (NIR) plateau are the main features of interest in the B spectrometer. There is close agreement based on the statistics performed between CIBR and LOWTRAN 7 with radiosonde input for both features. The shoulder height of the red edge is noticeably different in the regression method and the NIR plateau is almost featureless. CIBR and LOWTRAN 7 spectra show differences in the depth of the leaf water absorption features in the B spectrometer and the "real" depth cannot be resolved without ground measurements.

In the C spectrometer, CIBR and LOWTRAN 7 with radiosonde data are consistent when looking at the 1.45 μm cellulose and protein feature and the 1.7 μm cellulose and sugar absorption feature compared with the regression method and the LOWTRAN 7 ground input.

The 2.09 and 2.27 μm ligno-cellulose and 2.18 μm nitrogen absorption features in the D spectrometer are characterized well by CIBR, regression and both input modes of LOWTRAN 7. However, there is typically low signal to noise and this could affect results based on these absorption features.

For researchers who do not have access to ground based measurements of bright and dark targets at the time of the overflight, the LOWTRAN 7 and CIBR methods seem to provide reasonable alternatives.

Acknowledgements

This research was carried out at Jet Propulsion Laboratory, California Institute of Technology, Pasadena, California. The authors would like to thank Chris Elvidge of Desert Research Institute, Reno, Nevada for applying the regression data; Veronique Carrere, Steve Carpenter and Marit Jentoft-Nilsen, all of JPL, for their invaluable assistance; Dennis Joseph of National Center for Atmospheric Research (NCAR) for the radiosonde data; and Howard Veregin, UCSB, for instructions on how to be a "digi-slave" to produce the graphics.

References

Bruegge, C.J., J.E. Conel, J.S. Margolis, R.O. Green, G. Toon, V.E. Carrere, R.G. Holm, G. Hoover. 1990. In-Situ Atmospheric Water-Vapor Retrieval in Support of AVIRIS Validation, *Imaging Spectroscopy of the Terrestrial Environment,* Gregg Vane, Editor, Proc. SPIE 1298, Orlando, Florida, pp. 150-163.

Carrere, V.E. 1991. Use of High Spectral Resolution Airborne Visible/Infrared Imaging Spectrometer Data for Geologic Mapping: An Overview, *Physical Measurements and Signatures in Remote Sensing,* Fifth International Colloquium, Courcheval, France, International Society of Photogrammetry and Remote Sensing (in press).

Carrere, V.E., J.E. Conel, R.O. Green, C.J. Bruegge, J.S. Margolis, R.E. Alley. 1991. Analysis of Atmospheric Water Vapor Maps from AVIRIS at Salton Sea, California: Part I, Experiments, Methods, Results, and Error Budgets (unpublished).

Conel, J.E. and V.E. Carrere. 1991. Analysis of Atmospheric Water Vapor Maps from AVIRIS at Salton Sea, California: Part II, Surface Moisture Flux, Boundary Conditions and Plume Measurements (unpublished).

Conel, J.E., S. Adams, R.E. Alley, G. Hoover, S. Schultz. 1988. AIS Radiometry and the Problem of Contamination from Mixed Spectral Orders, *Remote Sensing of the Environment,* 24(1), pp. 179–200.

Curran, P.J. 1989. Remote Sensing of Foliar Chemistry, *Image Processing '89,* American Society for Photogrammetry and Remote Sensing, Sparks, Nevada, 23 May 1989, pp. 166-174.

Elvidge, C.D. 1988. Vegetation Reflectance Features in AVIRIS Data, *Proceedings of International Symposium on Remote Sensing of Environment, Sixth Thematic Conference, Remote Sensing for Exploration Geology,* ERIM, Houston, Texas, pp. 169-182.

Elvidge, C.D. and F.P. Portigal. 1990. Change Detection in Vegetation Using 1989 AVIRIS Data, *Imaging Spectroscopy of the Terrestrial Environment,* Gregg Vane, Editor, Proc. SPIE 1298, Orlando, Florida, pp. 178-189.

Green, R.O., V.E. Carrere, J.E. Conel. 1989. Measurement of Atmospheric Water Vapor Using the Airborne Visible/Infrared Imaging Spectrometer, *Image Processing '89,* American Society for Photogrammetry and Remote Sensing, Sparks, Nevada, 23 May 1989, pp. 31-44.

Kneizys, F.X., E.P. Shettle, G.P. Anderson, L.W. Abrew, J.H. Chetwynd, J.E.A. Shelby, W.O. Gallery. 1990. Atmospheric Transmittance/Radiance; Computer Code LOWTRAN 7, AFGL Hanscom AFB, MA.

van den Bosch, J.M. and R.E. Alley. 1990. Application of LOWTRAN 7 as an Atmospheric Correction to Airborne Visible/Infrared Imaging Spectrometer (AVIRIS) Data, *Remote Sensing Science for the Nineties,* 10th Annual International Geoscience and Remote Sensing Symposium, Washington, D.C., v. 1, pp. 175-178.

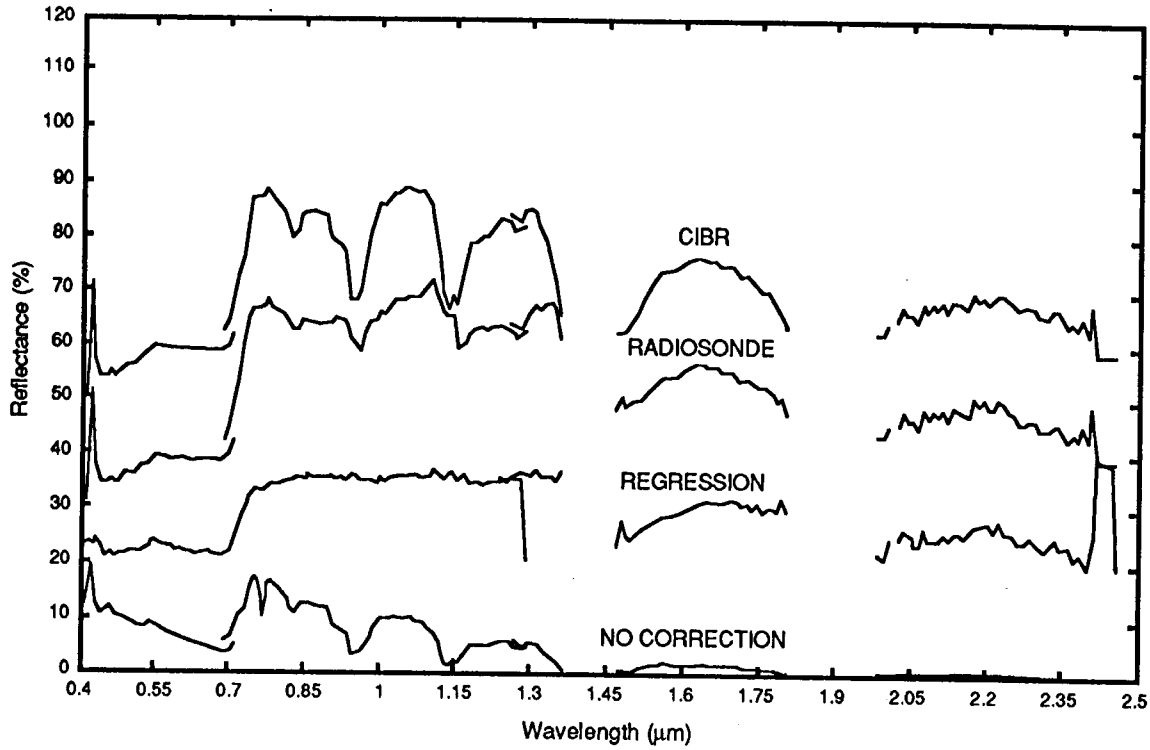

Figure 1. Irrigated Crop

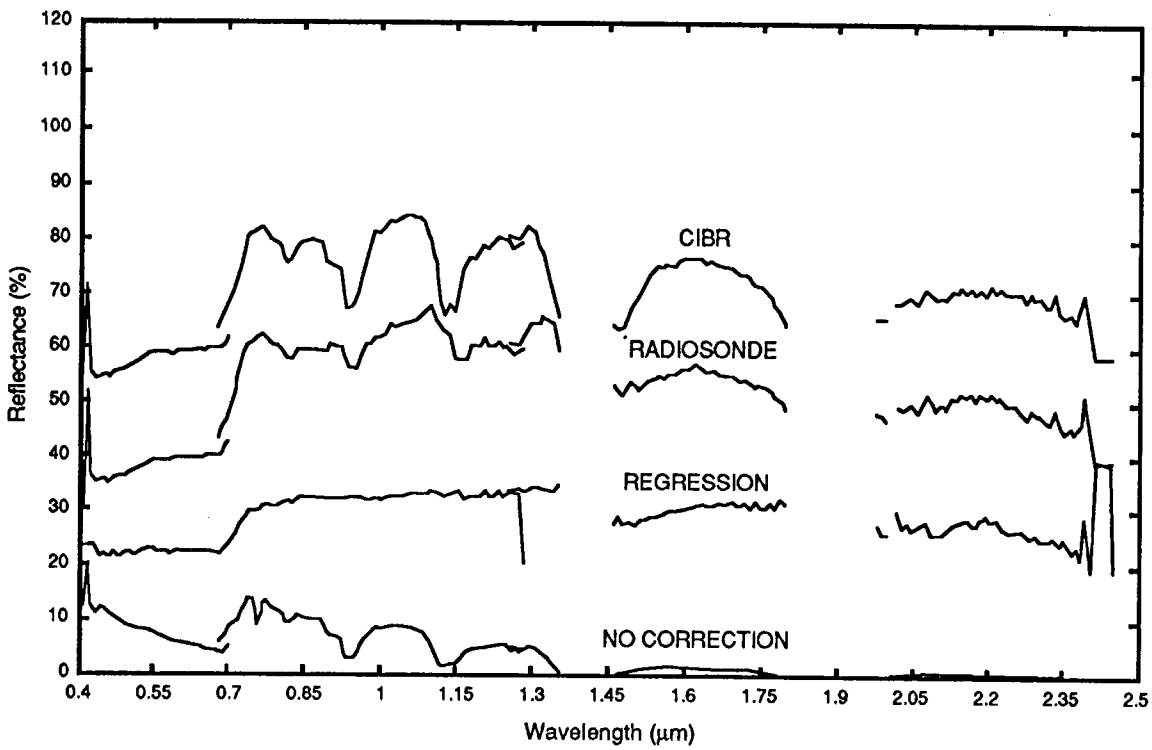

Figure 2. Chaparral

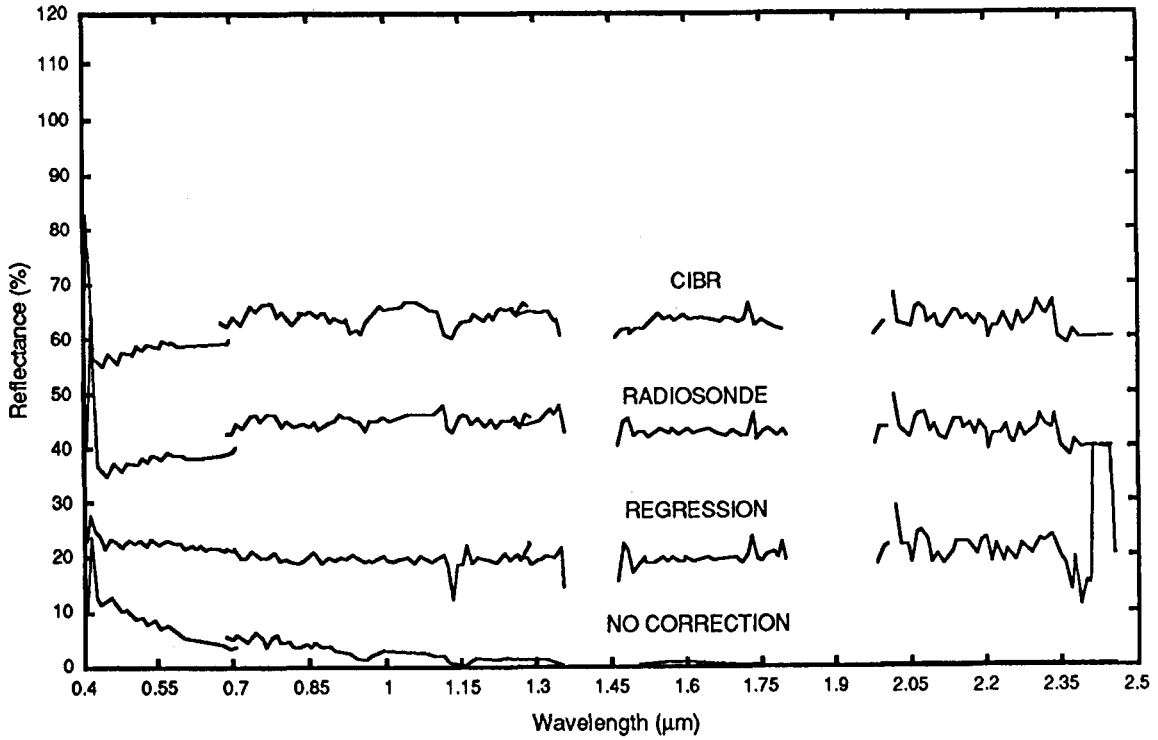

Figure 3. Water I

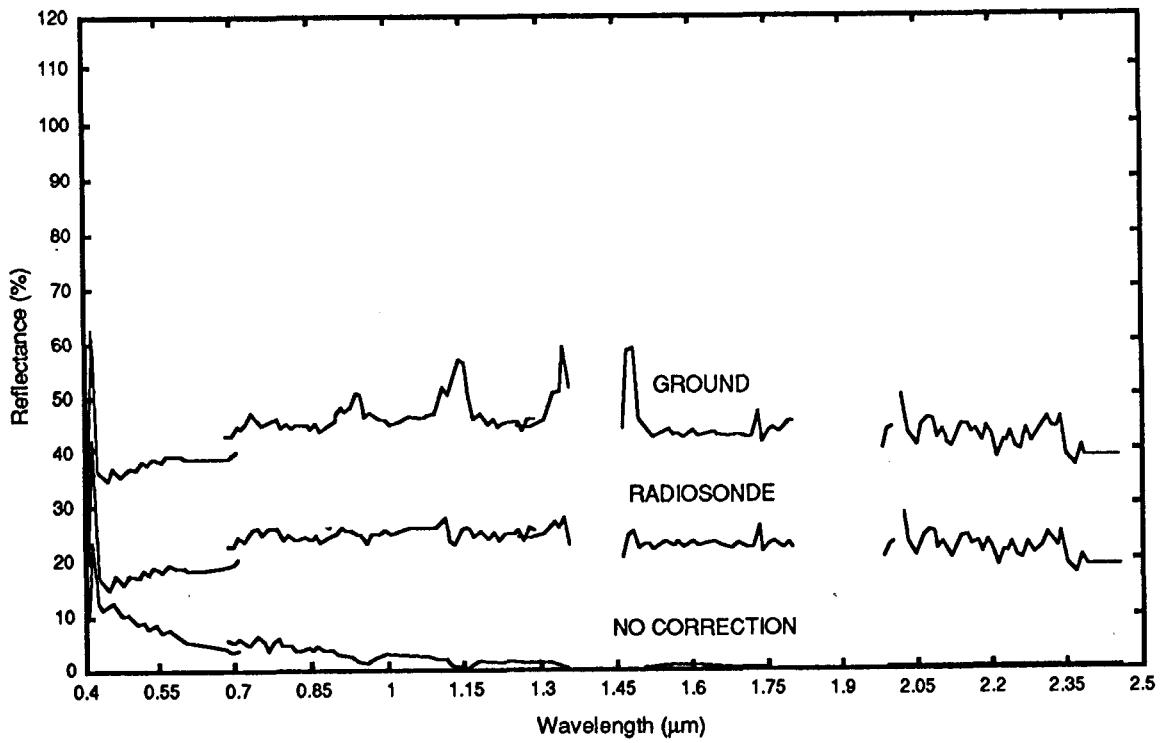

Figure 4. Water II

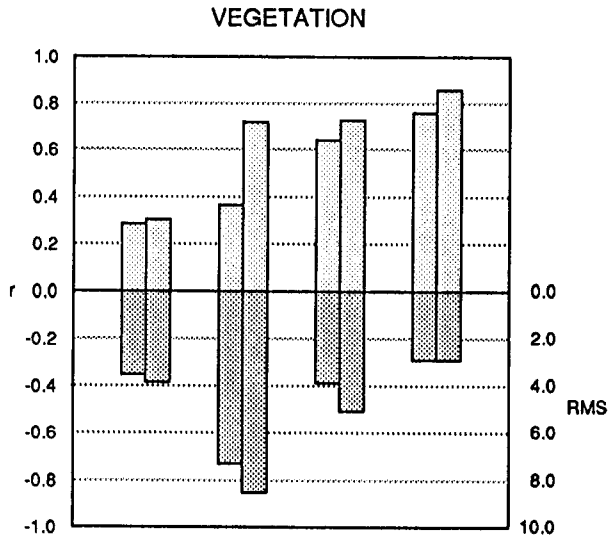

Figure 5a. Regression v. CIBR and LOWTRAN 7 with radiosonde

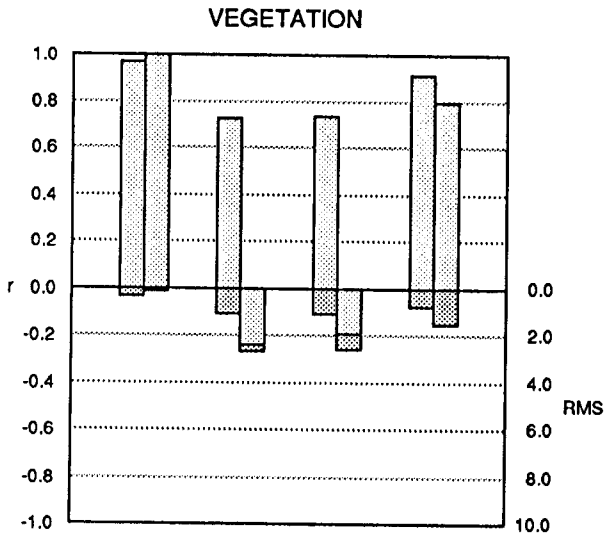

Figure 5b. CIBR v. LOWTRAN 7 with radiosonde and LOWTRAN 7 with ground inputs

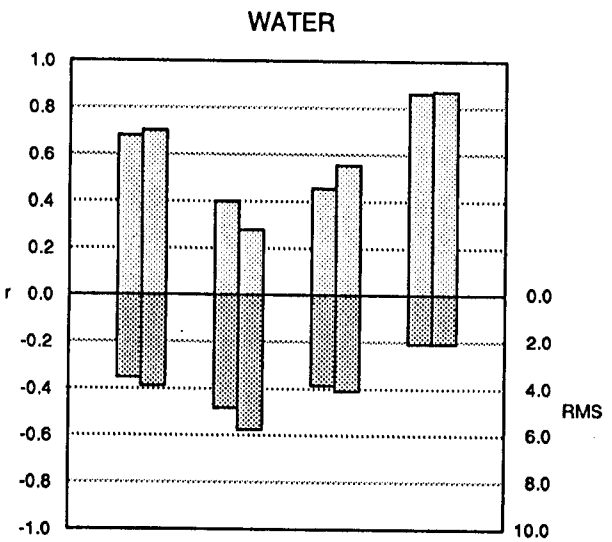

Figure 5c. Regression v. CIBR and LOWTRAN 7 with radiosonde

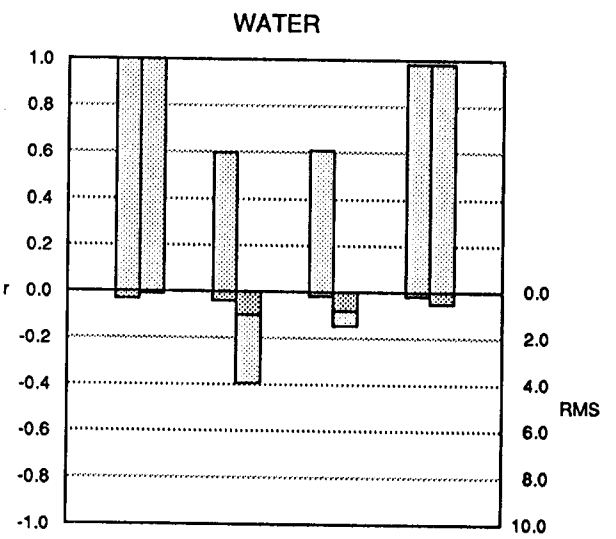

Figure 5d. CIBR v. LOWTRAN 7 with radiosonde and LOWTRAN 7 with ground inputs

Note: The four sets of bars in each graph represent spectrometers A, B, C, D. In Figures 5a and 5c, the first bar in each spectrometer is CIBR; the second bar is LOWTRAN 7 with radiosonde. In Figures 5b and 5d, the first bar in each spectrometer is LOWTRAN 7 with radiosonde input; the second bar is LOWTRAN 7 with ground data.

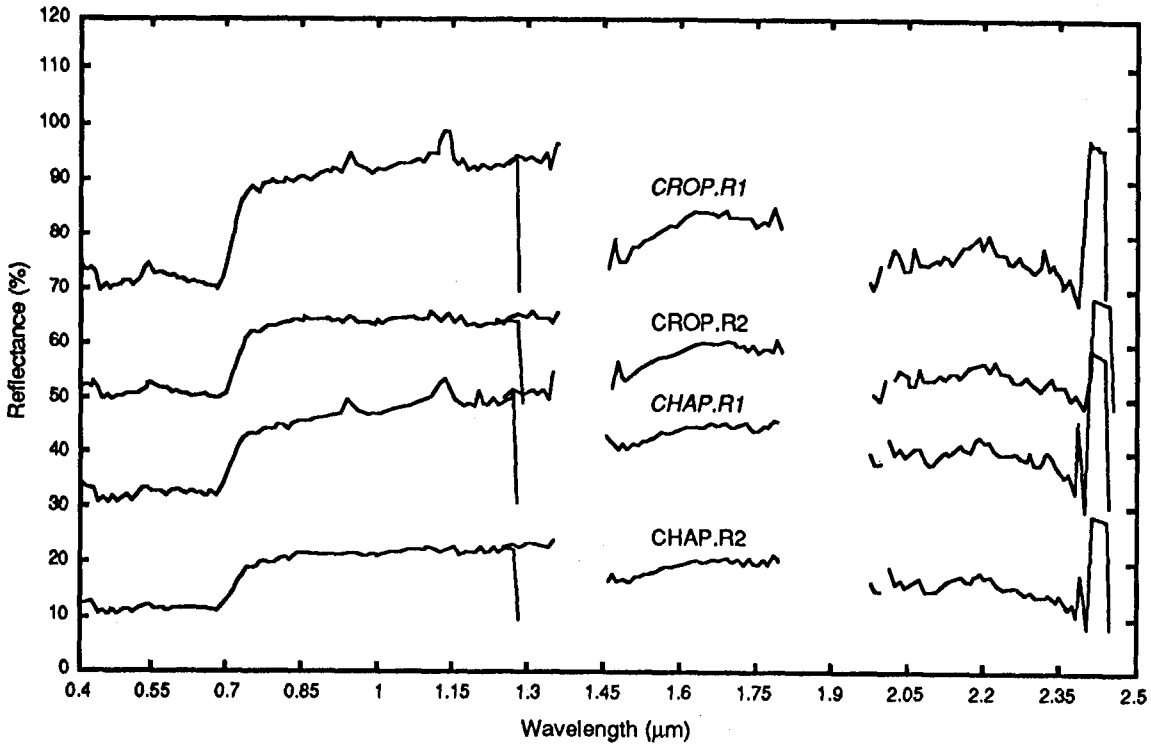

Figure 6. Comparison of two regression methods